

This article was downloaded by:

On: 29 January 2011

Access details: *Access Details: Free Access*

Publisher *Taylor & Francis*

Informa Ltd Registered in England and Wales Registered Number: 1072954 Registered office: Mortimer House, 37-41 Mortimer Street, London W1T 3JH, UK



Phosphorus, Sulfur, and Silicon and the Related Elements

Publication details, including instructions for authors and subscription information:

<http://www.informaworld.com/smpp/title~content=t713618290>

THE PHOSPHORYLATION OF 5,12-DIPHENYL-7,14-DIMETHYL-1,4,8,11-TETRAAZACYCLOTETRADECANE. AN NMR AND MOLECULAR MODELLING STUDY OF THE PARENT CYCLE AND THE REACTION PRODUCT

R. Boetzel^{ab}; S. Failla^c; P. Finocchiaro^c; G. Hägele^b

^a Institute of Food Research, Norwich, Great Britain ^b Institut für Anorganische Chemie und Strukturchemie I, Heinrich-Heine-Universität Düsseldorf, Düsseldorf, Germany ^c Facoltà di Ingegneria, Università di Catania, Catania, Italy

To cite this Article Boetzel, R. , Failla, S. , Finocchiaro, P. and Hägele, G.(1995) 'THE PHOSPHORYLATION OF 5,12-DIPHENYL-7,14-DIMETHYL-1,4,8,11-TETRAAZACYCLOTETRADECANE. AN NMR AND MOLECULAR MODELLING STUDY OF THE PARENT CYCLE AND THE REACTION PRODUCT', *Phosphorus, Sulfur, and Silicon and the Related Elements*, 104: 1, 71 – 80

To link to this Article: DOI: 10.1080/10426509508042579

URL: <http://dx.doi.org/10.1080/10426509508042579>

PLEASE SCROLL DOWN FOR ARTICLE

Full terms and conditions of use: <http://www.informaworld.com/terms-and-conditions-of-access.pdf>

This article may be used for research, teaching and private study purposes. Any substantial or systematic reproduction, re-distribution, re-selling, loan or sub-licensing, systematic supply or distribution in any form to anyone is expressly forbidden.

The publisher does not give any warranty express or implied or make any representation that the contents will be complete or accurate or up to date. The accuracy of any instructions, formulae and drug doses should be independently verified with primary sources. The publisher shall not be liable for any loss, actions, claims, proceedings, demand or costs or damages whatsoever or howsoever caused arising directly or indirectly in connection with or arising out of the use of this material.

THE PHOSPHORYLATION OF 5,12-DIPHENYL-7,14-DIMETHYL-1,4,8,11- TETRAAZACYCLOTETRADECANE. AN NMR AND MOLECULAR MODELLING STUDY OF THE PARENT CYCLE AND THE REACTION PRODUCT

R. BOETZEL,^{†‡} S. FAILLA,[§] P. FINOCCHIARO[§] and G. HÄGELE*[‡]

[‡]*Institut für Anorganische Chemie und Strukturchemie I, Heinrich-Heine-Universität Düsseldorf, Universitätsstr. 1, D-40225 Düsseldorf, Germany;*

[§]*Università di Catania, Facoltà di Ingegneria, Istituto Chimico, Viale A. Doria 6, I-95125 Catania, Italy*

Dedicated to Professor Roman Tyka on the occasion of his 70th birthday

(Received November 3, 1994; in final form February 7, 1995)

The NMR spectra of the reaction product **2** of 5,12-diphenyl-7,14-dimethyl-1,4,8,11-tetraazacyclotetradecane **1** and vinyl dimethylphosphonate under acidic conditions and the parent cycle **1** are subjected to a thorough analysis. The results in combination with molecular dynamics and geometry optimisations are used to determine the structure of **2**.

Key words: ¹H, ¹³C, 2D NMR, macrocycles, phosphorylation.

INTRODUCTION

Cyclam (1,4,8,11-tetraazacyclotetradecane) and its derivatives have found widespread interest as complexing agents for various applications. Introducing functional groups at carbon and nitrogen¹ leads to 'tailor-made' ligands with special properties, e.g. for the stabilisation of unstable oxidation states^{2–4} or high selectivity for a certain metal ion.⁵ Side chains introduced at the nitrogen atoms of cyclam and related compounds lead to an enhanced thermodynamic stability and kinetic inertness of complexes formed with these ligands; they have found applications as contrast agents for magnetic resonance imaging.⁶ A second field of application for N-functionalised tetraazamacrocycles is the development of labelled monoclonal antibodies for radioimmune diagnosis and therapy.^{7–9} Introducing phosphonate instead of carboxylate groups at nitrogen may open new possibilities for the design of potential complexing agents for both applications mentioned above.

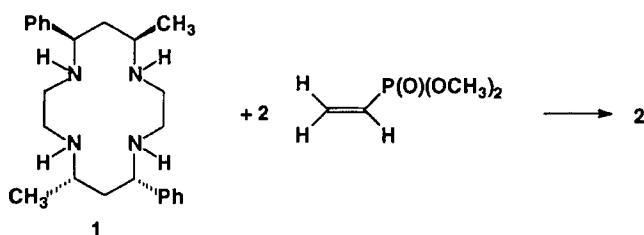
Two different approaches to macrocyclic ligands can be found: The first one comprises highly flexible ligands such as crown ethers or unsubstituted cyclams that are able to adopt a geometry suitable for complexation of a wide variety of metal ions easily. The second approach leads to the so-called pre-organised ligands where

[†]Part of forthcoming dissertation of R. Boetzel. Present address: Institute of Food Research, Norwich Research Park, Colney Lane, Norwich NR4 7UA, Great Britain.

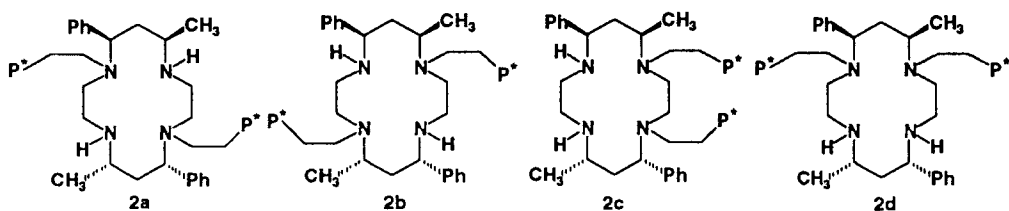
the geometry of the complex is already formed in the conformation of the macrocyclic ligand; it can be achieved introducing various substituents, e.g. in 5,5,7,12,12,14-hexamethyl-1,4,8,11-tetraazacyclotetradecane.^{10,11} Since in most cases the structure of a macrocyclic ligand in solution determines the structure of the complex to be formed, it should be possible to predict complexation properties of macrocycles by analysing their conformation in solution. The method of choice for this should be NMR spectroscopy in combination with molecular modelling.

THE PHOSPHORYLATION OF 1

To investigate the phosphorylation of a substituted cyclam, 5,12-diphenyl-7,14-dimethyl,1,4,8,11-tetraazacyclotetradecane **1**^{12–14} was chosen as a starting material.



The reaction of **1** with vinyl dimethylphosphonate in methanol under acidic catalysis leads to product **2** for which the presence of two phosphonate pendant arms was proved by elemental analysis. Unfortunately, it was not possible to get crystals for an X-ray analysis. Therefore, we tried to differentiate between the alternative structures **2a–2d** by NMR spectroscopy and molecular modelling.



RESULTS

NMR Spectroscopy

The numbering of protons and carbons for **1** and **2** is shown in Figure 1.

First, the macrocyclic rings of **1** and **2** shall be investigated.

For **1**, spectra at 200 MHz were used for the spectral analysis while for **2** the ¹H NMR spectrum which is shown in Figure 2 shows severe line overlap even at 600 MHz.

For assignment purposes, gradient-enhanced TOCSY (Figure 3) and HMQC H,C correlation spectra were recorded at 600 MHz.

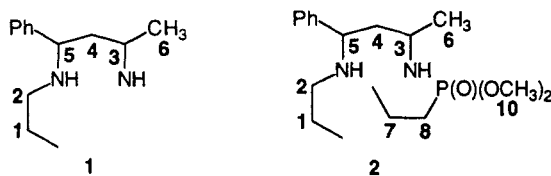


FIGURE 1 Numbering scheme for aliphatic protons and carbons of **1** and **2**.

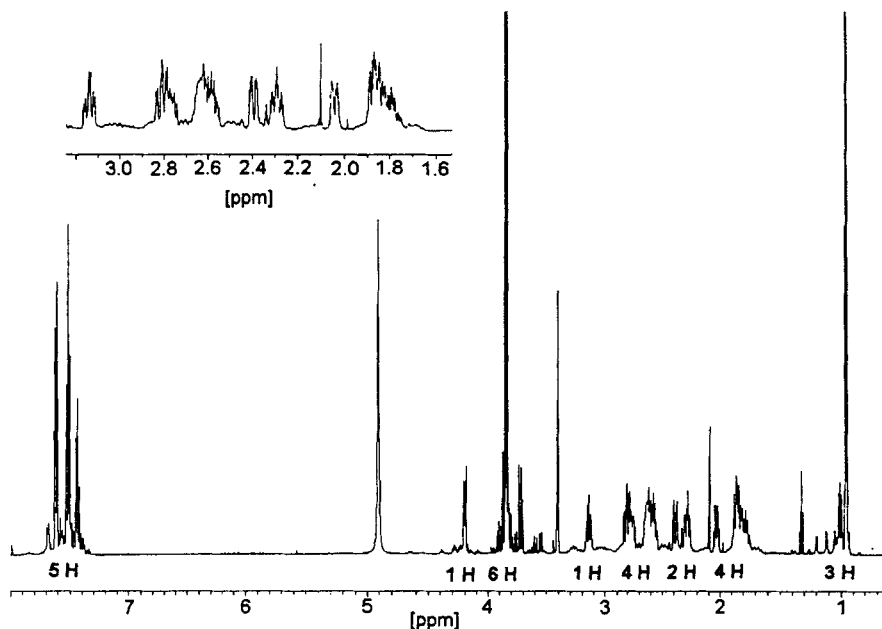


FIGURE 2 ^1H NMR spectrum of **2** (4% in CD_3OD , 600.132 MHz).

According to the ^1H and $^{13}\text{C}\{^1\text{H}\}$ NMR spectra, both macrocycles reveal an effective two-fold symmetry in solution; therefore, structures **2c** and **2d** can be ruled out since they would give rise to an unsymmetric spectral habitus.

The propylene (ABMNR₃ system) and ethylene (ABMN system) bridges of **1** and **2** can be analysed separately. Iterative refinement using program packages DAISY¹⁵ and PERCH¹⁶ leads to chemical shifts and coupling constants summarised in Tables I–IV.

The conformation of the ethylene bridges is derived from these results by applying a Karplus-type equation modified by Hawkins and Palmer.¹⁷ It allows the calculation of the dihedral angle N–C–C–N. For both compounds we find a gauche arrangement along both C–C bond; one of the two possible gauche rotamers (Figure 4) is exclusively populated in **1** and **2** at room temperature indicating a very stable structure.

The propylene units can be regarded as parts of rings formed by strong trans hydrogen bonding as observed quite frequently for fourteen-membered tetraaza-macrocycles. The most stable arrangement for the resulting rings is one where as

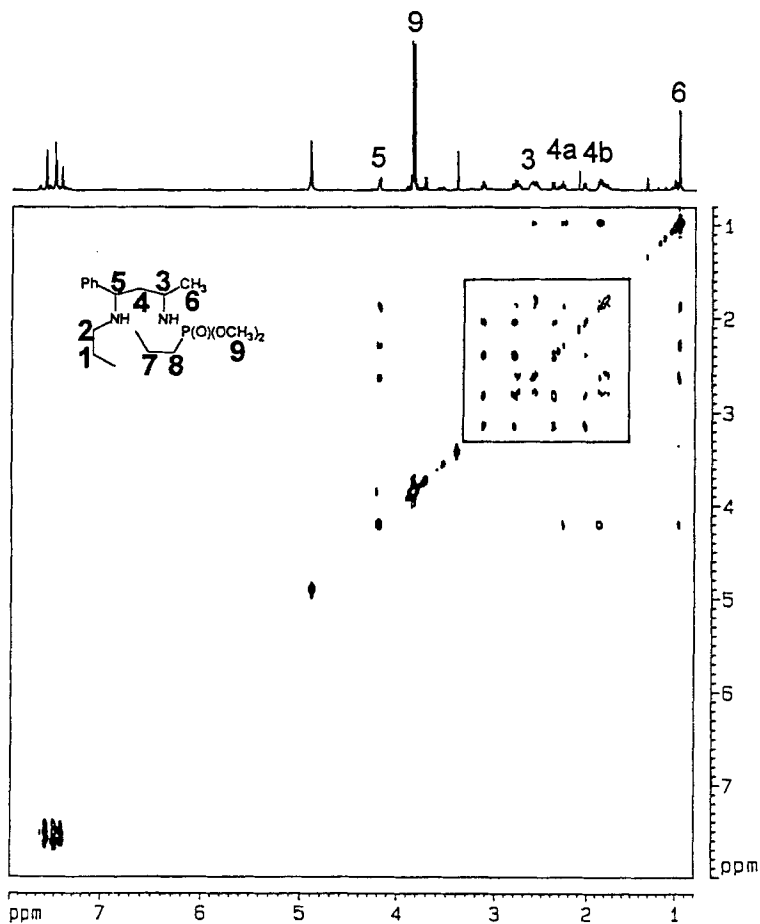


FIGURE 3 Aliphatic part of the gradient-enhanced TOCSY spectrum of **2** (4% in CD₃OD, 600.132 MHz); the assignment of the protons is indicated.

TABLE I

Chemical shifts [ppm vs. TMS; 4% in CD₃OD] of the protons in the propylene bridges of **1** and **2**

proton	3	4a	4b	5	6
1	3.007	1.803	1.693	3.767	1.112
2	2.638	2.289	1.868	4.196	0.966

TABLE II

H,H coupling constants [Hz; 4% in CD₃OD] in the propylene bridges of **1** and **2**

	3,4a	3,4b	3,6	4a,4b	4a,5	4b,5
1	10.4	1.9	6.3	-14.8	11.4	2.0
2	12.0	2.2	6.7	-14.4	10.2	4.2

TABLE III
Chemical shifts [ppm vs. TMS; 4% in CD₃OD] of the protons in the ethylene bridges of **1** and **2**

proton	1a	1b	2a	2b
1	2.892	2.448	2.634	2.377
2	3.138	2.041	2.810	2.392

TABLE IV
H,H coupling constants [Hz; 4% in CD₃OD] in the ethylene bridges of **1** and **2**

	1a,1b	1a,2a	1a,2b	1b,2a	1b,2b	2a,2b
1	-11.3	12.0	2.1	1.9	3.2	
2	-12.5	12.6	4.2	2.0	1.6	-14.4

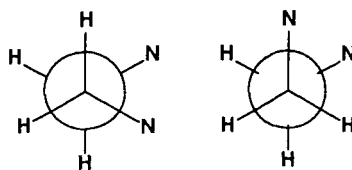


FIGURE 4 Two alternative gauche rotamers for the ethylene bridges in **1** and **2**.

TABLE V
Carbon-13 chemical shifts [ppm vs. TMS; 4% in CD₃OD] for the macrocyclic rings of **1** and **2**

carbon	1	2
1	49.01	43.93
2	48.80	42.51
3	67.76	53.32
4	47.21	43.29
5	67.71	58.08
6	21.30	13.59

many substituents as possible occupy the favoured equatorial positions. For both compounds, this trend is achieved as deduced from the coupling constants in Table II. Here we observe two large couplings representing axial interactions, and two small couplings resulting from an axial-equatorial relationship between the protons.

The ¹³C NMR data for the macrocyclic rings of **1** and **2** are shown in Table V.

Variable temperature ¹H and ¹³C NMR spectra for **1** show no significant changes in spectral appearance indicating the high stability for the dominant conformation of the macrocyclic rings.

Unfortunately, it was not possible to perform a thorough analysis of the ¹H NMR spectrum of **2** for the phosphonate groups; only chemical shifts (Table VI) were extracted due to severe line overlap and strong second order effects.

Since all measurements were performed in CD₃OD, coupling information across the nitrogen nuclei could not be exploited to determine the positions of the phos-

TABLE VI

¹H and ¹³C chemical shifts [ppm vs. TMS; 4% in CD₃OD], P,H and P,C coupling constants [Hz] for the phosphonate groups of **2**

proton		carbon	
7a	2.59	7	44.03 (4.3)
7b	2.57	8	24.49
8a	1.81	9a	53.52 (6.5)
8b	1.78	9b	53.51 (6.9)
9a	3.844 (10.9)		
9b	3.834 (10.8)		

phosphate groups. According to studies on ciliatin¹⁸ (2-aminoethane phosphonic acid) and derivatives,^{19,20} the antiperiplanar conformation along the C—C bond is favoured over gauche or eclipsed interactions. The same situation is expected for the bulky substituents in **2**.

Molecular Modelling

Molecular modelling is employed to distinguish between **2a** and **2b**. Two different approaches are taken into account: semiempirical (VAMP²¹) calculations using parameter sets AM1²² and PM3²³ as well as force field simulations (DISCOVER²⁴). Extensive calculations with and without solvent for **1** (methanol for VAMP, H₂O for DISCOVER, where no methanol parameters are included) show no significant differences for dihedral angles and energies between conformations in the presence or absence of solvation for this type of compounds. For **2**, force field calculations using water as a solvent lead to excessive computational times (several days); therefore, since semiempirical optimisation (VAMP) again showed no significant differences for conformers with and without solvent, no solvent effects were included for DISCOVER simulations of **2a** and **2b**.

Molecular dynamics (MD) calculations at 500 K were performed for **1**, **2a** and **2b** to search for minima in conformational space effectively. This 'temperature' cannot be compared to the physical concept of temperature; it is a means to provide the system with enough kinetic energy to overcome barriers of rotation or inversion to achieve conformational changes. To be able to compare data from molecular dynamics, a second set of calculations was performed at 300 K.

Using four representative minima from the 500 K MD simulations as input structures, the geometries of these conformers were optimised using semiempirical and force field programs to avoid misinterpretations resulting from errors of the methods themselves.

For **1** we find a very stable structure for the macrocyclic ring which is in accordance with the experimental data. Figure 5 shows one representative conformer of **1** calculated with VAMP (parameter set AM1) which agrees best with the NMR data.

According to the NMR results, a similar geometry should be found for the macrocyclic ring of **2**. The MD simulation for **2b** at 300 K reveals a stable arrange-

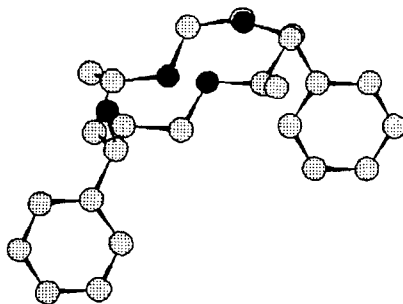


FIGURE 5 Most stable conformer of **1** calculated using VAMP with AM1 parameters.

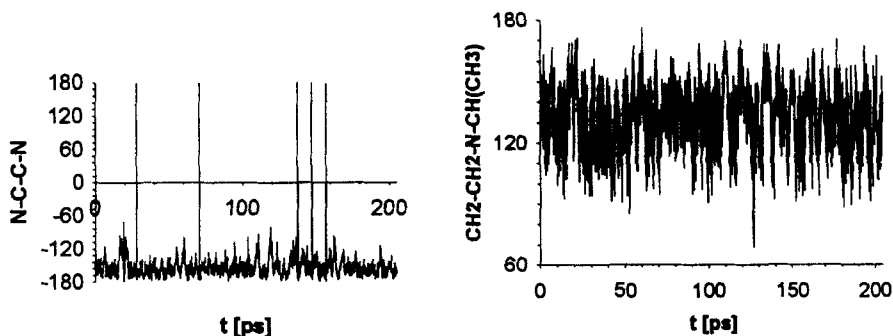


FIGURE 6 Time dependence of two dihedral angles in the macrocyclic ring of **2a**.

ment for the ring with gauche conformations for both ethylene bridges which is exactly the kind of structure supported by the coupling constants. For **2a**, a different situation arises: The MD simulation, which is most conveniently visualised in terms of changes of dihedral angles with time, the so-called trajectories, shows high conformational flexibility for the macrocyclic ring leading to the unfavourable antiperiplanar arrangement for the nitrogens in the ethylene bridges. Two representative trajectories are shown in Figure 6.

This conformational behaviour is in sharp contrast to the results extracted from the ^1H NMR spectrum. Therefore it is assumed that **2a** with substitution at the nitrogen atoms next to the phenyl groups is less favourable than **2b** with the phosphonate moieties in proximity to the less bulky CH_3 groups.

The hints found so far have to be supported by further results from geometry optimisations using semiempirical and force field programs. If the results from both different methods and parameter sets lead to the same conclusion as can be drawn from the MD simulations, there is strong proof for the existence of **2b** instead of **2a**.

The conformations of minimal energy resulting from optimisations with AM1 for **2a** and **2b** are shown in Figure 7.

The dihedral angles inside the macrocyclic ring of **2a** show that significant deviations from the stable structure of the parent cycle **1** exist, e.g., antiperiplanar arrangement for the nitrogens in the ethylene bridges and an unfavourable gauche conformation along the C—C bonds in the phosphonate groups. Table VII summarises some of the relevant torsion angles of **1**, **2a** and **2b**.

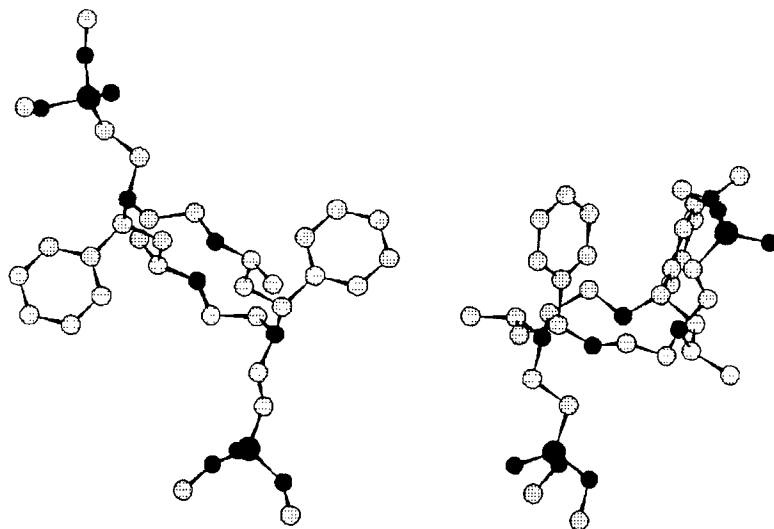


FIGURE 7 Conformations of minimal energy resulting from optimisations with AM1 for **2a** (left) and **2b** (right).

TABLE VII
Relevant torsion angles (AM1) for the macrocyclic rings of **1**, **2a** and **2b**

dihedral angle	1	2a	2b
N-C-C ₁ -N ₁	54.1	-162.9	65.8
C-C ₁ -N ₁ -C ₂	156.3	91.1	-173.0
N ₂ -C ₅ -C ₆ -N ₃	60.8	148.8	65.7

Since all methods and parameter sets lead to comparable results, it can be assumed that the differences in conformation between **2a** and **2b** do not stem from the methods themselves but reflect inherent properties of the molecules. Therefore **2b** represents the most stable structure for the bis-phosphorylated product **2**.

CONCLUSIONS

It is shown that a combination of NMR spectroscopy and molecular modelling proved to be useful for the structural elucidation of **2**. This method provides a means for an effective search for potential complexing agents.

EXPERIMENTAL

Synthesis

The parent macrocycle **1** was prepared according to Hideg and Lloyd.¹

To 5.2 g (0.0137 mol) of **1** dissolved in methanol (150 ml) at room temperature were added 10 g (0.0735 mol) of vinyl dimethylphosphonate and a few drops of acetic acid. The reaction mixture was

allowed to react under stirring at reflux temperature in an N₂ atmosphere for 22 hours. Evaporation of the solvent under reduced pressure yielded an oil to which 50 ml of dry diethyl ether were added. This mixture was left overnight in a refrigerator. At -15°C very slowly a crystalline white powder was obtained, filtered off and dried, yielding 1.75 g (20%) of **2**, m.p. 180–185°C. Several recrystallisations from methanol gave white crystals, m.p. 185–187°C.

³¹P{¹H} NMR: 20.39 ppm (s)

Elemental analysis: C₃₂H₅₄N₄O₆P₂ (652.73 g/mol) calculated: C 58.88, H 8.34, N 8.58%; found: C 58.91, H 8.38, N 8.49%

NMR Measurements

If not mentioned otherwise, ¹H, ³¹P{¹H} and ¹³C{¹H} and 2D NMR measurements were performed on degassed and sealed samples on Bruker AM 200 and AMX 600 spectrometers at room temperature. Methanol-d₄ was used as an internal lock; ¹H and ¹³C{¹H} NMR spectra were referenced against internal TMS; 85% H₃PO₄ served as an external standard for ³¹P. 2D NMR spectra were recorded in TPPI mode with 2K points in f₁ and 512 t₁ increments.

Iterative refinement of ¹H NMR spectra was achieved using the program packages DAISY (version for Bruker X32), LAO-PC and PERCH.

Molecular Modelling

The molecular structure simulations were performed on a Silicon Graphics Indigo workstation (INSIGHT/DISCOVER) and on a main frame CONVEX C220 (VAMP 4.4).

Molecular dynamics were performed at 300 and 500 K with 20 ps heating time for 300 ps. For the force field minimisation in water, a layer of 20.0 Å in diameter was laid around the molecule and minimisation was done with conjugate gradients (rms < 0.01). The semiempirical VAMP calculations followed the reaction field theory using AM1 and PM3 approximations with keywords PRECISE, SCRF AM1/PM3, CAVITY = 1.2, MEHF.

ACKNOWLEDGEMENTS

Financial support by the Fonds der Chemischen Industrie (G.H.), Italian C.N.R. and M.V.R.S.T.(P.F.) is gratefully acknowledged. Thanks are due to Dipl.-Chem. K. Kreidler for introduction into the programs VAMP and DISCOVER as well as for many helpful hints, and Dr. M. Ackermann, Bruker Analytische Meßtechnik, Rheinstetten, for the possibility to use the AMX 600 spectrometer.

REFERENCES

1. T. A. Kaden, *Adv. Supramol. Chem.*, **3**, 65 (1993).
2. D. C. Olson and J. Vasilevskis, *Inorg. Chem.*, **8**, 1611 (1969).
3. I. J. Clark and J. M. Harrowfield, *Inorg. Chem.*, **23**, 3740 (1984).
4. M. Pesavento, A. Profumo, T. Soldi and L. Fabbrizzi, *Inorg. Chem.*, **24**, 3873 (1985).
5. R. D. Hancock and A. E. Martell, *Chem. Rev.*, **89**, 1875 (1989).
6. A. D. Sherry *et al.*, *J. Magn. Res.*, **76**, 528 (1988).
7. T. A. Kaden, *Nachr. Chem. Tech. Lab.*, **38**, 728 (1990).
8. L. Yuanfang and W. Chuanchu, *Pure & Appl. Chem.*, **63**, 427 (1991).
9. D. Parker, *Chem. Soc. Rev.*, **19**, 271 (1990).
10. R. Boetzel, S. Failla, P. Finocchiaro and G. Hägele, *Magn. Res. Chem.*, in press.
11. B.-F. Liang, *Tunghai Xuebao*, **23**, 267 (1982); *CA* **98**, 178603.
12. K. Hideg and D. Llyod, *J. Chem. Soc. (C)*, 3441 (1971).
13. R. W. Hay and P. M. Gidney, *J. Chem. Soc., Dalton Trans.*, 975 (1976).
14. G. Ferguson, P. Roberts, D. Lloyd and K. Hideg, *J. Chem. Soc., Chem. Commun.*, 149 (1977).
15. G. Hägele, M. Engelhardt and W. Boenigk, "Simulation und automatisierte Analyse von Kernresonanzspektren," VCH Weinheim, 1987.
16. R. Laatikainen, *J. Magn. Res.*, **92**, 1 (1991).
17. C. J. Hawkins and J. A. Palmer, *Coord. Chem. Rev.*, **44**, 1 (1982).
18. M. Ackermann, R. Boetzel, N. Christin, F. Hammerschmidt, G. Hägele and C. Rabiller, to be published.

19. R. Boetzel and G. Hägele, *Phosphorus, Sulfur & Silicon*, **77**, 312 (1993).
20. R. Boetzel and G. Hägele, unpublished results.
21. VAMP Vers. 4.4, vectorised version for CONVEX C220.
22. M. J. S. Dewar, E. G. Zoebisch, E. F. Healy and J. J. P. Stewart, *J. Am. Chem. Soc.*, **107**, 3902 (1985).
23. J. J. P. Stewart, *J. Comput. Chem.*, **10**, 209 (1989).
24. BIOSYM Technologies, Inc., 10065 Barnes Canyon Road, San Diego, CA 92121, USA.